The near-resonant regimes of a moving load in a 3D problem for a coated elastic half space

B. Erbaş
Dept. of Mathematics, Anadolu University, Eskişehir, Turkey

J. Kaplunov[1]
School of Computing and Mathematics, Keele University, Staffordshire, ST5 5BG, UK

D. A. Prikazchikov
School of Computing and Mathematics, Keele University, Staffordshire, ST5 5BG, UK

O. Şahin
Dept. of Mathematics, Anadolu University, Eskişehir, Turkey

Abstract
The paper deals with 3D analysis of the near-resonant regimes of a point load, moving steadily along the surface of a coated elastic half-space. The developed approach relies on a specialized hyperbolic-elliptic formulation for the wave field earlier established by the authors. Straightforward integral solutions of the 2D perturbed wave equation describing wave propagation along the surface are derived along with their far-field asymptotic expansions obtained using the uniform stationary phase method. Both sub-Rayleigh and super-Rayleigh cases are studied. It is shown that the singularities arising at the contour of the Mach cones typical of the super-Rayleigh case, are smoothed due to a dispersive effect of the coating.

Keywords
3D elasticity, moving load, Rayleigh wave, thin coating, uniform asymptotics.

1 Introduction

Various modern industrial applications, including substantial development of the high-speed train operation, enhance significantly the importance of 3D modeling of elastic structures under moving loads, see e.g. Cao et al. [1]. Moving load problems have been analyzed for more than a century now, see Fryba [2] and references therein. Among the numerous publications on the subject most of the contributions were carried out within 2D framework. A very few analytical studies dealing with 3D problems were mainly oriented to numerical evaluation of exact solutions expressed in an integral form. As an example, we mention the developments in Georgiadis and Lukotrafitis [3] using the Radon transform.

In this paper we adapt the asymptotic methodology based on extracting the contribution of the Rayleigh wave to the overall dynamic response. A specialized formulation for a near surface wave field initially derived the for plane strain problem (Kaplunov et al. [4]) has been later on generalized to the 3D setup taking into account the effect of a thin coating (Dai et al. [5]) The cited papers develop a perturbation scheme starting from the presentation of the Rayleigh wave eigensolutions in terms of arbitrary harmonic functions, see Chadwick [6], Kiselev and Parker [7]. In this case the decay over the interior is governed by elliptic equations for elastic potentials, whereas surface wave propagation is described by a hyperbolic equation, which is singularly perturbed by a pseudo-differential operator in presence of a coating. The developed hyperbolic-elliptic model has been applied first to a transient

[1]**Corresponding author:**
School of Computing and Mathematics, Keele University, Staffordshire, ST5 5BG, UK.
Email: j.kaplunov@keele.ac.uk

2D moving load problem (Kaplunov et al. [8]) providing drastic simplification to resonant analysis and enabling a qualitative insight into transient dynamic phenomena. An explicit 3D steady-state solution for a moving load on elastic half-space has been also recently obtained, see Kaplunov et al. [9].

Below we consider the near-resonant regimes of a point load, steadily moving along the surface of a coated half-space. The previous considerations dealing with layered structures (Achenbach et al. [12], Kalinchuk et al. [13]) usually have had little focus on resonant phenomena. The presented 3D treatment extends results of the above mentioned publications, Kaplunov et al. [9], and also a more recent paper of Kaplunov et al. [14], investigating a steady state plane strain problem for a coated half-space. The studied problem has two small parameters, one of which is associated with the proximity of the speed of the moving load to the resonant Rayleigh wave speed, whereas another one originates from a small thickness of the coating. Scaling, incorporating the effect of both these parameters is found. Analysis of the super-Rayleigh regime reveals Mach cones similar to those in case of an uncoated half-space Kaplunov et al. [9], which are now smoothed due to a dispersive effect of the coating. A relatively simple integral solution is subject to asymptotic analysis in the far-field using the uniform stationary phase method. The leading order asymptotic behaviour is expressed in terms of the Fresnel functions. The implementation of the causality principle is also addressed in application to a dispersive surface wave. For the sub-Rayleigh regime we also develop uniform asymptotic procedure resulting in the leading order asymptotic behaviour given by the Airy function.

The paper is organized as follows. Section 2 contains statement of the problem, followed by the proposed asymptotic scaling. The super-Rayleigh regime of the moving load is analyzed in Section 3, whereas the final Section 4 deals with the sub-Rayleigh mode. Numerical comparisons of exact and asymptotic results are presented for both cases.

2 Statement of the problem and scaling

Consider 3D linear elastodynamics of a half-space ($-\infty < x_1, x_2 < \infty$, $0 \le x_3 < \infty$) coated by a thin layer ($-\infty < x_1, x_2 < \infty$, $-h \le x_3 \le 0$) under concentrated vertical force of magnitude P moving at a constant speed c along the line $x_2 = 0$ of the surface $x_3 = -h$, see Fig. 1.

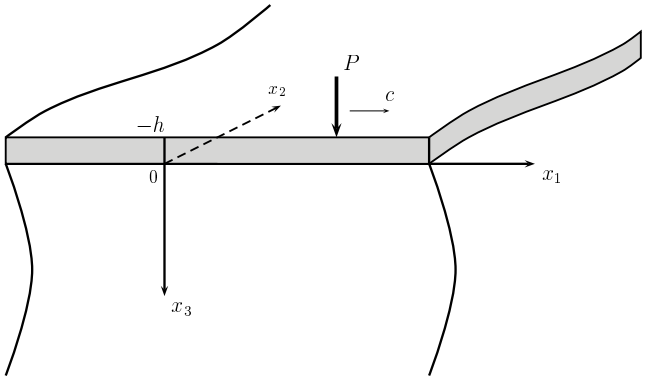

Figure 1: Coated half-space under moving load.

We start from the approximate elliptic-hyperbolic formulation for the Rayleigh wave field in a coated half-space proposed in Dai et al. [5]. Within the latter the decay over the interior of the half-space is described by pseudo-static elliptic equations for elastic potentials

$$\frac{\partial^2 \phi}{\partial x_3^2} + k_1^2 \Delta_2 \phi = 0, \qquad \frac{\partial^2 \psi_i}{\partial x_3^2} + k_2^2 \Delta_2 \phi = 0, \qquad i = 1, 2 \tag{2.1}$$

where

$$\Delta_2 = \frac{\partial^2}{\partial x_1^2} + \frac{\partial^2}{\partial x_2^2}, \qquad k_i = \left(1 - \frac{c_R^2}{c_i^2}\right)^{1/2},$$

with c_1, c_2, and c_R denoting the longitudinal, shear, and Rayleigh wave speeds, respectively.

The displacement vector $\mathbf{u} = (u_1, u_2, u_3)$ is expressed through the potentials as

$$\mathbf{u} = \operatorname{grad}\phi + \operatorname{curl}\psi, \qquad \psi = (-\psi_2, \psi_1, 0). \tag{2.2}$$

The wave propagation along the plane $x_3 = 0$ is governed by the singularly perturbed hyperbolic equation

$$\Delta_2\phi - \frac{1}{c_R^2}\frac{\partial^2\phi}{\partial t^2} - bh\sqrt{-\Delta_2}\Delta_2\phi = AP\delta(x_1 - ct)\delta(x_2), \tag{2.3}$$

and the relations

$$\frac{\partial\phi}{\partial x_i} = \frac{2}{1+k_2^2}\frac{\partial\psi_i}{\partial x_3}, \qquad i = 1, 2. \tag{2.4}$$

Here b, and A are constants, depending on the material parameters of the half-space and the coating, and $\sqrt{-\Delta_2}$ is a pseudo-differential operator, for more details see Dai et al. [5]. The sign of the coefficient b is crucial for the type (max or min) of the phase speed at zero wave number, see Shuvalov and Every [10], and also Dai et al. [5].

The sought for approximation of the Rayleigh wave field over the half-space follows from the solution of the formulated problem (2.1), (2.3) and (2.4). The derivation is considerably simplified in case of the tangential displacements along the plane $x_3 = 0$, which are expressed from (2.2) and (2.4) as

$$u_i = \frac{c_R^2}{2c_2^2}\frac{\partial\phi}{\partial x_i}, \quad i = 1, 2. \tag{2.5}$$

Below we restrict ourselves to the steady-state regime. On introducing the moving coordinate $\lambda = x_1 - ct$, we get from (2.3) for the sub-Rayleigh ($c < c_R$) and super-Rayleigh ($c > c_R$) cases

$$\frac{\partial^2\phi}{\partial x_2^2} + \varepsilon^2\frac{\partial^2\phi}{\partial\lambda^2} - bh\sqrt{-\left(\frac{\partial^2}{\partial x_2^2} + \frac{\partial^2}{\partial\lambda^2}\right)}\left(\frac{\partial^2\phi}{\partial x_2^2} + \frac{\partial^2\phi}{\partial\lambda^2}\right) = AP\delta(\lambda)\,\delta(x_2) \tag{2.6}$$

and

$$\frac{\partial^2\phi}{\partial x_2^2} - \varepsilon^2\frac{\partial^2\phi}{\partial\lambda^2} - bh\sqrt{-\left(\frac{\partial^2}{\partial x_2^2} + \frac{\partial^2}{\partial\lambda^2}\right)}\left(\frac{\partial^2\phi}{\partial x_2^2} + \frac{\partial^2\phi}{\partial\lambda^2}\right) = AP\delta(\lambda)\,\delta(x_2), \tag{2.7}$$

respectively, where

$$\varepsilon = \left|1 - \frac{c^2}{c_R^2}\right|^{1/2}. \tag{2.8}$$

The adapted model is oriented to the analysis of a near-resonant response dominated by the Rayleigh wave contribution and is valid provided that $\varepsilon \ll 1$, see Kaplunov et al. [9], and Kaplunov et al. [8]. It also assumes that the thickness of the coating h is small compared to a typical wavelength, see Dai et al. [5]. The presence of two small parameters in the equations (2.6) and (2.7) leads to two different types of degeneration, at $\varepsilon = 0$ and at $h = 0$, corresponding to the critical speed of the load coinciding with the Rayleigh wave speed, and an uncoated half-space, respectively. This observation motivates the scaling

$$\lambda = \frac{\xi bh}{\varepsilon^2}, \qquad x_2 = \frac{\eta bh}{\varepsilon^3}, \tag{2.9}$$

which defines an elongated domain over $\left(x_2h^{-1}, \lambda h^{-1}\right)$ plane, see Fig. 2. Using this scaling, the equations (2.6) and (2.7) become

$$\frac{\partial^2\phi}{\partial\eta^2} - \frac{\partial^2\phi}{\partial\xi^2} - \sqrt{-\frac{\partial^2}{\partial\xi^2}}\,\frac{\partial^2\phi}{\partial\xi^2} = \frac{AP}{\varepsilon}\delta(\xi)\,\delta(\eta) \tag{2.10}$$

and

$$\frac{\partial^2\phi}{\partial\eta^2} + \frac{\partial^2\phi}{\partial\xi^2} - \sqrt{-\frac{\partial^2}{\partial\xi^2}}\,\frac{\partial^2\phi}{\partial\xi^2} = \frac{AP}{\varepsilon}\delta(\xi)\,\delta(\eta), \tag{2.11}$$

respectively.

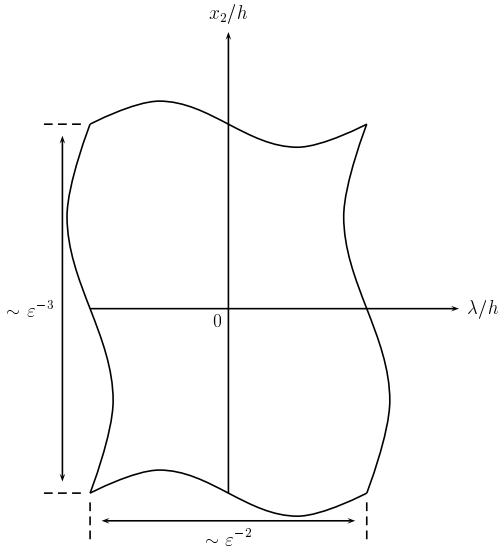

Figure 2: Asymptotic scaling.

3 Super-Rayleigh regime

Let us study first equation (2.10). On applying the Fourier transform in variable ξ, we obtain

$$\frac{d^2\phi^F}{d\eta^2} + k^2(1+|k|)\phi^F = \frac{AP}{\varepsilon}\delta(\eta), \tag{3.1}$$

where

$$\phi^F(k,\eta,0) = \int_{-\infty}^{\infty} \phi(\xi,\eta,0)\, e^{-ik\xi} d\xi. \tag{3.2}$$

Bearing in mind the symmetry of the sought for solution in η, we get

$$\phi^F = \frac{AP}{\varepsilon} \frac{\sin\left(|k|\sqrt{1+|k|}|\eta|\right)}{|k|\sqrt{1+|k|}}. \tag{3.3}$$

The related inverse transform is given by

$$\phi(\xi,\eta,0) = \frac{AP}{\pi\varepsilon} \int_0^{\infty} \frac{\sin\left(k\sqrt{1+k}|\eta|\right)\cos(k\xi)}{k\sqrt{1+k}} dk. \tag{3.4}$$

The tangential displacements along the plane $x_3 = 0$ are expressed through the last integral by formula (2.5). The analysis is rather similar for both displacements, hence we deal with u_1 only. It can be written as

$$u_1(\xi,\eta,0) = \frac{APc_R^2\varepsilon}{4\pi b h c_2^2} \sum_{n=1}^{2} I_n(\xi,\eta) \tag{3.5}$$

where

$$I_n(\xi,\eta) = \mathrm{sgn}(\xi) \int_0^{\infty} \frac{\cos\left(|\xi| h_n(k)\right)}{g(k)} dk, \qquad n = 1,2, \tag{3.6}$$

with

$$g(k) = \sqrt{1+k}, \qquad h_n(k) = k\left[g(k)\mu - (-1)^n\right], \qquad \mu = \left|\frac{\eta}{\xi}\right|.$$

Let us investigate the far-field asymptotic behaviour of the oscillating integrals (3.6) as $|\xi| \gg 1$, assuming $\mu \sim 1$. It may be shown that the effect of the first integral I_1 is asymptotically minor, whereas I_2 is dominated by the contribution of the stationary point of $h_2(k)$, given by

$$k_* = \frac{2\left(1 - 3\mu^2 + \sqrt{3\mu^2+1}\right)}{9\mu^2}. \tag{3.7}$$

Note that at the contour of the Mach cone $\mu = 1$ ($|\xi| = |\eta|$) the stationary point $k_* = 0$ coincides with the lower limit of the integral I_2. Therefore, we have to apply the uniform stationary phase method, e.g. see Borovikov [11] and references therein, having at leading order

$$I_2 \sim \mathrm{Re}\left[\frac{e^{i|\xi|h_*}}{g_*}\int\limits_0^\infty e^{\frac{1}{2}i|\xi|h''(k_*)(k-k_*)^2}dk\right], \tag{3.8}$$

where

$$h_* = h(k_*) = \frac{2\left(1 - 3\mu^2 + \sqrt{3\mu^2+1}\right)\left(\sqrt{3\mu^2+1} - 2\right)}{27\mu^2}, \tag{3.9}$$

and

$$g_* = g(k_*) = \frac{1+\sqrt{3\mu^2+1}}{3\mu}. \tag{3.10}$$

The resulting displacement u_1 is then given by

$$u_1 \sim \frac{AP\varepsilon c_R^2 k_*}{4\pi b h c_2^2 g_* a}\frac{\mathrm{sgn}(\xi)}{|\xi|^{1/2}}F(|\xi|,\mu), \tag{3.11}$$

where

$$F(|\xi|,\mu) = \cos\left[h_*|\xi|\right]\left\{\sqrt{\frac{\pi}{8}} - \mathrm{C}\left(a\sqrt{|\xi|}\right)\right\} - \sin\left[h_*|\xi|\right]\left\{\sqrt{\frac{\pi}{8}} - \mathrm{S}\left(a\sqrt{|\xi|}\right)\right\}, \tag{3.12}$$

with

$$a = -k_*\sqrt{\frac{h''(k_*)}{2}} = \frac{\left[3\mu^2 - 1 - \sqrt{3\mu^2+1}\right]\sqrt[4]{3\mu^2+1}}{3\mu\left[1+\sqrt{3\mu^2+1}\right]}, \tag{3.13}$$

and $S(x)$ and $C(x)$ are the Fresnel functions, defined by

$$S(x) = \int\limits_0^x \sin(x^2)dx, \qquad C(x) = \int\limits_0^x \cos(x^2)dx, \tag{3.14}$$

see e.g. Abramowitz and Stegun [15]. It is pretty obvious that the derived uniform asymptotic formula is also valid at $\mu > 1$ when $k_* < 0$ and a takes imaginary values.

The interpretation of the formulae in this section written in terms of $|\xi|$ and $|\eta|$ relies on the implementation of the causality principle. In absence of a coating, when $h = 0$, equation (2.10) degenerates to the wave equation. For the latter it is logical to deal with the Mach cones behind the load only, i. e. at $\xi > 0$ for $b > 0$ and $\xi < 0$ for $b < 0$, as follows from scaling (2.9), see Fig 3. At the same time the full solution of the associated original problem in 3D elasticity will contain the contribution of faster

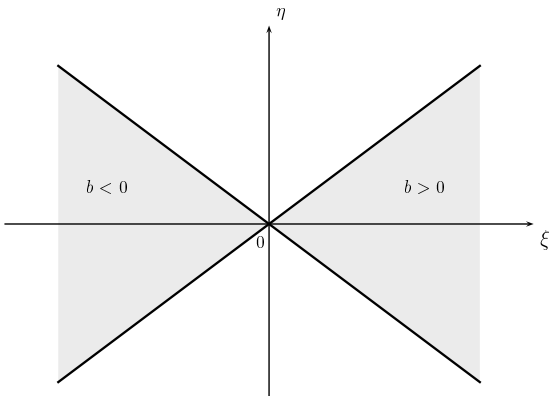

Figure 3: Mach cones

compression and shear waves ignored within the framework of the adapted specialized formulation, see Section 1. As a result, the question of taking into consideration both Mach cones (behind and in front of the load) may be apparently raised. To certain extent this may be relevant to the phenomenon of a head shear wave propagating faster than a cylindrical shear wave in case of the plane Lamb problem, e. g. see Poruchikov [16].

Another interesting feature is concerned with a dispersive nature of the analyzed surface wave governed by a singularly perturbed wave equation. In this case due to causality we seemingly have to require decay of the solution outside the interior of the Max cones predicted by the related degenerate non-dispersive equation. The asymptotic behaviours of the Fresnel functions in (3.12) at the large imaginary values of the argument Abramovitz and Stegun [15] show that the function (3.12) is exponentially small at $\mu - 1 \gg |\xi|^{-1}$.

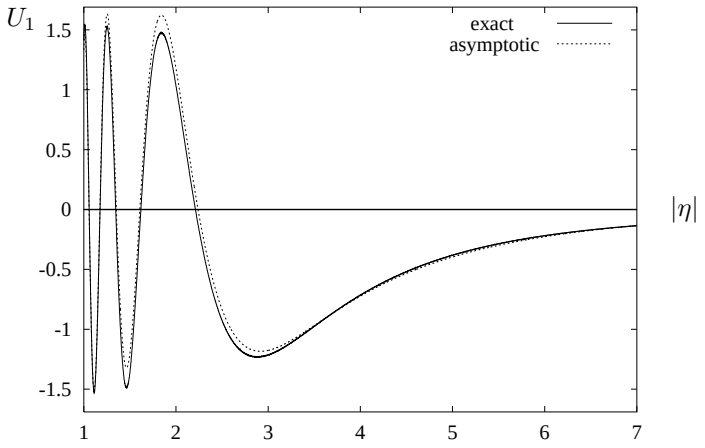

Figure 4: Profile of the super-Rayleigh displacement U_1 at $|\xi| = 5$.

Numerical illustrations of the scaled longitudinal displacement

$$U_1 = \frac{4\pi bhc_2^2}{APc_R^2\varepsilon}u_1 \tag{3.15}$$

are presented in Figs. 4 and 5, containing longitudinal and transverse cross-sections of the profile, respectively. On these plots the results of numerical integration of (3.5) are depicted by solid lines, with the dotted line corresponding to the asymptotic approximation (3.11). The Fig. 4 shows dependence of

U_1 on the transverse variable $|\eta|$, with calculations performed for the value of $|\xi| = 5$. The next Fig. 5 is mirroring the previous Fig. 4, depicting variation of U_1 on $|\xi|$, with calculations performed for $|\eta| = 5$.

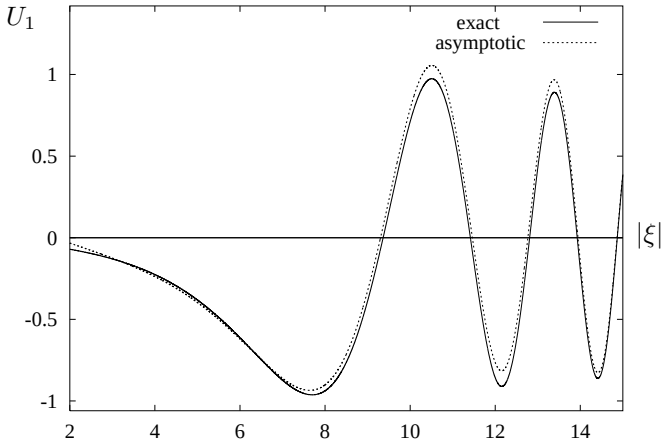

Figure 5: Profile of the super-Rayleigh displacement U_1 at $|\eta| = 5$.

It is clearly seen from both Figs. 4 and 5, that the dispersive effect of the coating causes smoothing of the discontinuities along the lines $|\xi| = |\eta|$, arising in an uncoated half-space, see Kaplunov et al. [9]. The oscillations occur within the Mach cone, decaying away from it. The period of oscillations diminish on both graphs as $\mu \to 0$, due to $h_* \to \infty$, as may be noticed from (3.9).

The asymptotic formula (3.11) provides a surprisingly accurate approximation of the solution (3.5), which is applicable even at not very large values of the parameter $|\xi|$, used on Figs. 4 and 5. This is due to the fact that the argument of the Fresnel functions $a\sqrt{|\xi|} \sim |\xi|^{1/2}\mu^{-1}$ in (3.12), therefore we actually operate with a larger parameter $|\xi|\mu^{-2}$.

In order to provide a better overview of the investigated wave phenomena, we present a 3D illustration of a part of the scaled displacement profile, corresponding to exact integral solution (3.5), see Fig. 6.

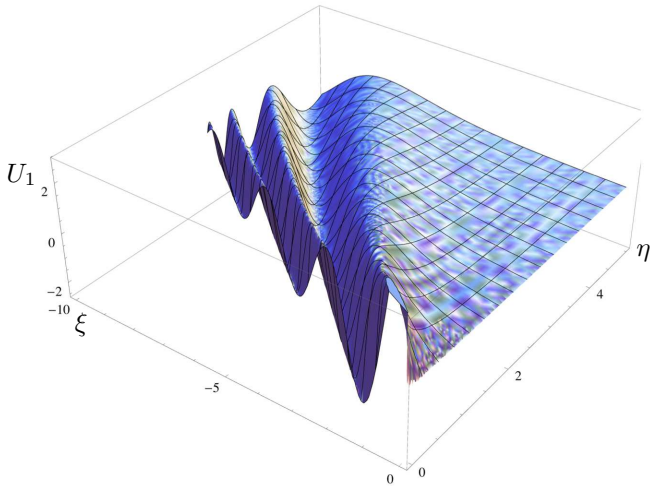

Figure 6: A 3D profile of the longitudinal super-Rayleigh displacement U_1.

4 Sub-Rayleigh regime

Let us now study equation (2.11). On applying the Fourier transform, we get

$$\frac{d^2\phi^F}{d\eta^2} - k^2(1-|k|)\phi^F = \frac{AP}{\varepsilon}\delta(\eta). \tag{4.1}$$

The solution of this equation is piecewise in the parameter $|k|$. Due to symmetry in η along with decay at infinity, it may be written as

$$\phi^F(k,\eta,0) = \begin{cases} -\dfrac{AP}{\varepsilon}\dfrac{e^{-|k|\sqrt{1-|k|}|\eta|}}{|k|\sqrt{1-|k|}}, & |k|<1; \\ \\ \dfrac{AP}{\varepsilon}\dfrac{\sin\left(|k|\sqrt{|k|-1}|\eta|\right)}{|k|\sqrt{|k|-1}}, & |k|>1. \end{cases} \tag{4.2}$$

Then, we have for the longitudinal displacement along the plane $x_3 = 0$

$$u_1(\xi,\eta,0) = \frac{AP\varepsilon c_R^2 \mathrm{sgn}(\xi)}{2\pi c_2^2 bh}\left[\int_0^1 \frac{e^{-k\sqrt{1-k}|\xi|\mu}}{\sqrt{1-k}}\sin(k|\xi|)\,dk - \int_1^\infty \frac{\sin\left(k\sqrt{k-1}|\xi|\mu\right)}{\sqrt{k-1}}\sin(k|\xi|)\,dk\right] \tag{4.3}$$

Consider the far-field approximation ($|\xi| \gg 1$). It can be verified that the leading order asymptotic behaviour of u_1 is given by contribution of the stationary points arising from the second integral in (4.3). Changing the variable k to $t = \sqrt{k-1}$, this integral takes the form

$$\int_1^\infty \frac{\sin\left(k\sqrt{k-1}|\eta|\right)}{\sqrt{k-1}}\sin(k|\xi|)\,dk = \sum_{n=1}^{2} G_n(|\xi|,\mu), \tag{4.4}$$

where

$$G_n(|\xi|,\mu) = (-1)^{n+1}\int_0^\infty \cos\left[|\xi|(t^2+1)(t\mu+(-1)^n)\right]dt. \tag{4.5}$$

In this case only the first integral G_1 possesses stationary points. They are

$$t_* = \frac{1\pm\sqrt{1-3\mu^2}}{3\mu}, \qquad 0<\mu\le\frac{1}{\sqrt{3}}, \tag{4.6}$$

which coincide along the line $\mu = \dfrac{1}{\sqrt{3}}$ ($|\xi| = \sqrt{3}|\eta|$). This again motivates making use of the uniform stationary phase method, giving

$$\begin{aligned} G_1(|\xi|,\mu) &= \mathrm{Re}\left\{e^{ip|\xi|}\int_0^\infty e^{i|\xi|\mu\left[\left(t-\frac{1}{3\mu}\right)^3+3^{1/3}\mu^{-2/3}q\left(t-\frac{1}{3\mu}\right)\right]}dt\right\} \\ &= \frac{2\pi}{\sqrt[3]{3\mu|\xi|}}\cos(p|\xi|)\,\mathrm{Ai}\left(q|\xi|^{2/3}\right), \end{aligned} \tag{4.7}$$

where

$$p = \frac{2(9\mu^2+1)}{27}, \qquad q = \frac{3\mu^2-1}{(3\mu)^{4/3}}, \tag{4.8}$$

and

$$\mathrm{Ai}(z) = \frac{1}{\pi}\int_0^\infty \cos\left(\frac{t^3}{3}+zt\right)dt \tag{4.9}$$

is the Airy function, see Abramowitz and Stegun [15].

The resulting far-field asymptotic expansion for the longitudinal displacements takes the form

$$u_1 \sim -\frac{AP\varepsilon c_R^2 \mathrm{sgn}(\xi)}{c_2^2 bh \sqrt[3]{3|\xi|\mu}} \cos\left(p|\xi|\right) \mathrm{Ai}\left(q|\xi|^{2/3}\right). \tag{4.10}$$

Numerical illustrations on Figs. 7, 8, using the scaled displacement

$$U_1 = \frac{bhc_2^2}{APc_R^2\varepsilon} u_1, \tag{4.11}$$

demonstrate the comparisons of the exact solution (4.3) with its far-field asymptotic approximation (4.10), depicted as previously by solid and dotted lines, respectively.

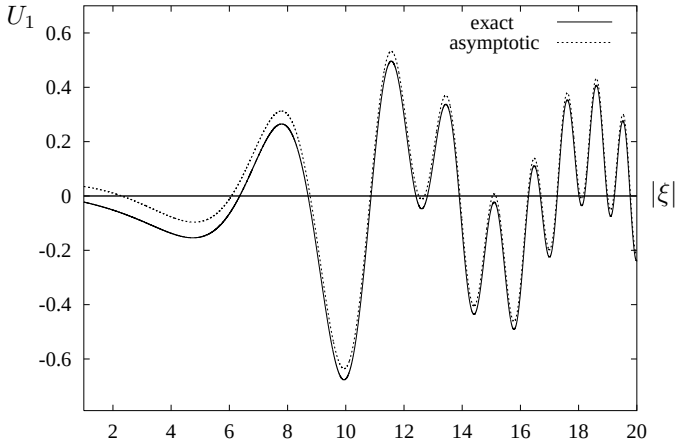

Figure 7: Longitudinal cross-section of the sub-Rayleigh displacement profile at $|\eta| = 5$.

The calculations of Figure 7 are performed for fixed value of $|\eta| = 5$, with Figure 8 showing a perpendicular cross-section at $|\xi| = 10$. It may be observed from Figs. 7 and 8 that even though there is no Mach cone

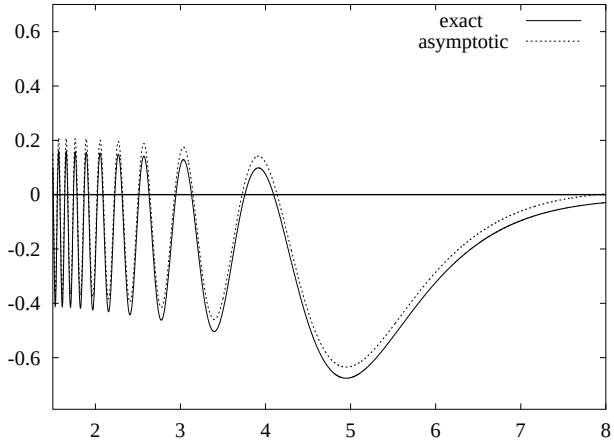

Figure 8: Transverse cross-section of the sub-Rayleigh displacement profile U_1 at $|\xi| = 10$.

in the sub-Rayleigh regime, there is still a region of oscillations associated with $\mu < \dfrac{1}{\sqrt{3}}$. The period of oscillations decrease as $\mu \to 0$. In the region $\mu > \dfrac{1}{\sqrt{3}}$ the profile demonstrates exponential decay.

Concluding this section, we present a 3D numerical illustration of the scaled displacement U_1 defined in (4.11) over the region $-10 \leq \xi \leq 0$, $0 \leq \eta \leq 5$ see Fig. 9.

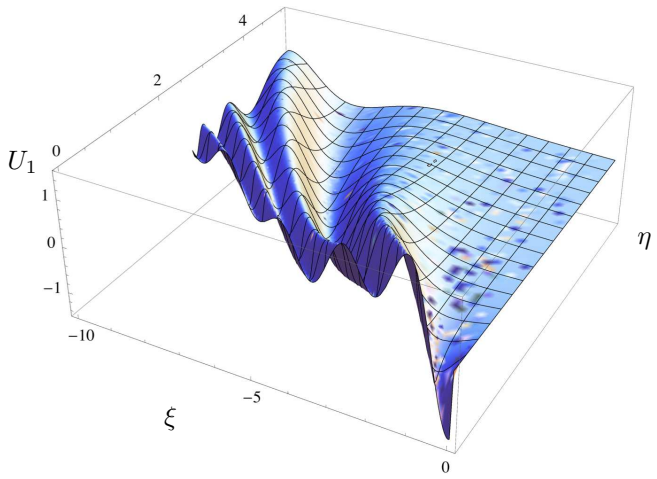

Figure 9: A 3D profile of the longitudinal sub-Rayleigh displacement U_1 (4.11)

Concluding remarks

The adapted specialized long wave model oriented to the surface wave field induced by a moving load on a coated half-space seems to be optimal for analyzing the resonant phenomena. It enables to simplify all the derivations significantly due to ignoring the contribution of compression and shear bulk waves. In addition, this model makes a more straightforward qualitative insight, including, for example, discussion of the causality principle in application to a dispersive surface wave.

Scaling taking into consideration the degenerations characteristic of near-resonant regimes and a small thickness of the coating is determined. Simple integral solutions of the 2D scaled equation governing the surface motion, are derived both for sub- and super-Rayleigh cases. The associated wave field over the interior can be relatively easily restored by solving analytically or numerically standard boundary value problems for pseudo-static elliptic equations.

Uniform far-field asymptotic behaviours expressed through the Airy function and Fresnel integrals are established. They can be useful for investigating the transition regions along the surface. For the super-Rayleigh regime such a region is associated with the contour of a Mach cone. As might be expected, the presence of a coating results in smoothing of the singularities arising in the related problem for an uncoated half-space.

Acknowledgement

The support of the Research project of Anadolu University, No: 1306F268 is gratefully acknowledged. JK and DAP would also like to thank Prof C.J. Chapman for fruitful discussions of the causality principle.

References

1. Cao Y, Xia H, and Li Z. A semi-analytical/FEM model for predicting ground vibrations induced by high-speed train through continuous girder bridge. J. Mech. Sci. Technol. 2012; 26 (8): 2485–2496.

2. Fryba L. Vibration of solids and structures under moving loads. 3th ed. London: Thomas Telford, 1999.

3. Georgiadis HG and Lykotrafitis G. A method based on the Radon transform for three-dimensional elastodynamic problems of moving loads. J. Elast. 2001; 65: 87–129.

4. Kaplunov J, Zakharov A and Prikazchikov DA. Explicit Models for Elastic and Piezoelastic Surface Waves. IMA J. Appl. Math. 2006; 71: 768–782.

5. Dai HH, Kaplunov J, and Prikazchikov DA. A Long-Wave Model for The Surface Elastic Wave in A Coated Half-Space. Proc. R. Soc. London, Ser. A 2010; 466: 3097–3116.

6. Chadwick P. Surface and Interfacial Waves of Arbitrary Form in Isotropic Media. J. Elast 1976; 6: 73–80.

7. Kiselev AP and Parker DF. Omni-Directional Rayleigh, Stoneley and Scholte Waves with General Time Dependence. Proc. R. Soc. London, Ser. A 2010; 466: 2241–2258.

8. Kaplunov J, Nolde E and Prikazchikov DA. A Revisit to the Moving Load problem Using An Asymptotic Model for The Rayleigh Wave. Wave Motion. 2010; 47: 440–451.

9. Kaplunov J, Prikazchikov DA, Erbaş B and Şahin O. On a 3D Moving Load Problem for An Elastic Half Space. Wave Motion 2013; 50: 1229–1238.

10. Shuvalov AL and Every AG On the long-wave onset of dispersion of the surface-wave velocity in coated solids. Wave Motion 2008; 45: 857?863.

11. Borovikov VA. Uniform Stationary Phase Method. London: Inspec/Iee, 1994.

12. Achenbach JD, Keshava SP, Herrmann G. Moving load on a plate resting on an elastic half-space. J. of Appl. Mech. 1967; 34 (2): 910–914.

13. Kalinchuk VV, Belyankova TI, Schmid G, Tosecky A. Dynamic of layered half space under the action of moving and oscillating load. Bull. South. Res. Cent. RAS. 2005; 1 (1): 3-11.

14. Kaplunov J, Oblakova TV and Prikazchikov DA. Near-resonant regimes of a moving load in the plane-strain problem for a coated elastic half-space. Matematicheskoe Modelirovanie i Chislennye Metody. 2014; 1.1: 57-67.

15. Abramowitz M and Stegun IA. Handbook of Mathematical Functions: with Formulas, Graphs, and Mathematical Tables. New York: Dover Publications, 2012.

16. Poruchikov VB. Methods of the classical theory of elastodynamics. Berlin: Springer-Verlag, 1992.